Optical manipulation of self-aligned graphene flakes in liquid crystals

Christopher W. Twombly,[1] Julian S. Evans,[1] and Ivan I. Smalyukh[1,2,3,*]

[1]*Department of Physics and Liquid Crystal Materials Research Center, University of Colorado, Boulder, Colorado 80309, USA*

[2]*Department of Electrical, Computer, and Energy Engineering and Materials Science Engineering Program, University of Colorado, Boulder, Colorado 80309, USA*

[3]*Renewable and Sustainable Energy Institute, National Renewable Energy Laboratory and University of Colorado, Boulder, Colorado 80309, USA*

[*] *ivan.smalyukh@colorado.edu*

Abstract: Graphene recently emerged as a new two-dimensional material platform with unique optical, thermal and electronic properties. Single- or few-atom-thick graphene flakes can potentially be utilized to form structured bulk composites that further enrich these properties and enable a broad range of new applications. Here we describe optical manipulation of self-aligned colloidal graphene flakes in thermotropic liquid crystals of nematic and cholesteric types. Three-dimensional rotational and translational manipulation of graphene flakes by means of holographic optical tweezers allows for non-contact spatial patterning of graphene, control of liquid crystal defects, and low-power optical realignment of the liquid crystal director using these flakes. Potential applications include optically- and electrically-controlled reconfigurable liquid crystalline dispersions of spontaneously aligning colloidal graphene flakes and new electro-optic devices with graphene-based interconnected transparent electrodes at surfaces and in the bulk of liquid crystals.

11. M. R. Jones, R. J. Macfarlane, B. Lee, J. Zhang, K. L. Young, A. J. Senesi, and C. A. Mirkin, “DNA-nanoparticle superlattices formed from anisotropic building blocks,” Nat. Mater. **9**(11), 913–917 (2010).
12. P. M. Chaikin and T. C. Lubensky, *Principles of Condensed Matter Physics* (Cambridge University Press, 1995).
13. M. Zapotocky, L. Ramos, P. Poulin, T. C. Lubensky, and D. A. Weitz, “Particle-stabilized defect gel in cholesteric liquid crystals,” Science **283**(5399), 209–212 (1999).
14. M. Ravnik, G. P. Alexander, J. M. Yeomans, and S. P. Žumer, “Three-dimensional colloidal crystals in liquid crystalline blue phases,” Proc. Natl. Acad. Sci. U.S.A. **108**(13), 5188–5192 (2011).
15. D. Engström, R. P. Trivedi, M. Persson, K. A. Bertness, M. Goksör, and I. I. Smalyukh, “Three-dimensional imaging of liquid crystal structures and defects by means of holographic manipulation of colloidal nanowires with faceted sidewalls,” Soft Matter **7**(13), 6304–6312 (2011).
16. R. P. Trivedi, D. Engström, and I. I. Smalyukh, “Optical manipulation of colloids and defect structures in

are not encountered in conventional isotropic fluids and colloidal dispersions [11,12]. These interactions and the ensuing self-assembled and self-aligned structures can be further tailored by controlling the chirality of the host LC medium [13–15], the shape of the colloids [6,7,15,16], the boundary conditions for the director **n** (describing local average orientation of mesogenic molecules) at the LC-colloid interface [1,10], and the long-range patterns of molecular alignment **n**(**r**) in the surrounding LC. The latter can be switched by electric and magnetic fields, light, temperature, and mechanical stimuli, potentially enabling reconfigurable self-assembled colloidal structures. In addition to spherical colloids, LC-mediated interactions have been explored for particles with anisotropic shapes such as prolate

of [3-(trimethoxysilyl)propyl]octadecyl-dimethylammonium chloride (DMOAP, purchased from Aldrich), rinsed with deionized water, and dried with compressed nitrogen gas. For planar alignment, a solution of 3 wt. % of polyimide PI-2555 in N-methyl-2-pyrrolidone (both obtained from HD Microsystems) was first filtered with a 10 μm particulate filter and spun coat onto the cleaned glass plates for 30 seconds at 400 rpm and, subsequently, for 1 min at 1500 rpm. The coated glass substrates were pre-baked at 110° C for 10 minutes to remove the solvent and then baked at 250° C for two hours to fully crosslink the polyimide. The substrates were subsequently rubbed with velvet cloth in a unidirectional fashion to set the direction of the easy axis for the planar LC alignment. The glass plates of both

influence on orientation of the flake with respect to the far-field director $\mathbf{n_0}$, which is different from the case of much thicker lithographically generated colloidal platelets [6], but similar to about 5nm-thick polygonal gold platelets [7]. In cholesteric LCs with pitch p ≈5μm, comparable to the lateral flake size, we find flakes aligning parallel to the uniformly twisting director **n** and perpendicular to the helical axis **χ** (Figs. 1 and 2). FCPM and PM observations reveal that most of the flakes are suspended in the LC bulk for long periods of time (months) while undergoing Brownian motion (Figs. 1-3), although some flakes (~5%) sediment to surfaces.

The surface anchoring of the director **n** at graphene-LC interfaces is tangential due to pi-stacking [21] and not perturbed by flake edges, which is natural given that the thickness of graphene flakes is comparable or smaller than the LC molecular size. Therefore, a graphene flake of diameter D imposes an easy axis for the alignment of $\mathbf{n}(\mathbf{r})$ tangential to its surfaces. Using the Rapini-Papoular surface anchoring potential [12], one finds that the surface energy due to deviation of a small flake with D < 500nm for an angle θ from its equilibrium orientation parallel to $\mathbf{n_0}$ is $F_s = (\pi W D^2/4)\sin^2\theta$, where W is the polar surface anchoring coefficient. Using $W \approx 10^{-5}$ J/m^2 [21], one finds that $F_s >> k_B T$ even for flakes of D ~100nm barely observable in an optical microscope and at relatively small θ, explaining well defined self-alignment of the graphene flakes parallel to $\mathbf{n_0}$. As the flake size increases to D ≥ K/W ≈500 nm and larger, the alignment effects become even stronger and dominated by elasticity, where $K = (K_{11} + K_{22} + K_{33})/3$ is the average elastic constant (Table 1) and K_{11}, K_{22}, and K_{33} are splay, twist, and bend Frank elastic constants, respectively.

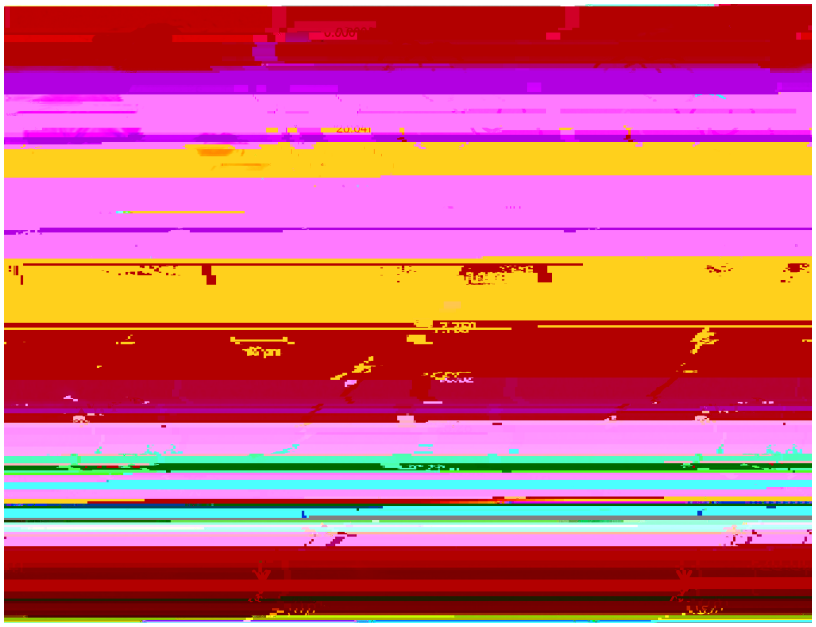

Fig. 1. Optical manipulation of graphene flakes in liquid crystals. (a) An optical micrograph of typical graphene flakes in immersion oil produced from cleaved highly ordered graphite; the folds and changes in layer thickness are visible as changes in optical transmission through the

Table 1. Material parameters of the used nematic LCs.

	K_{11}, pN	K_{22}, pN	K_{33}, pN	K, pN	n_o	n_e
5CB	6.4	3	10	≈7	1.536	1.714
ZLI-2806	14.9	7.9	15.4	≈11	1.475	1.518

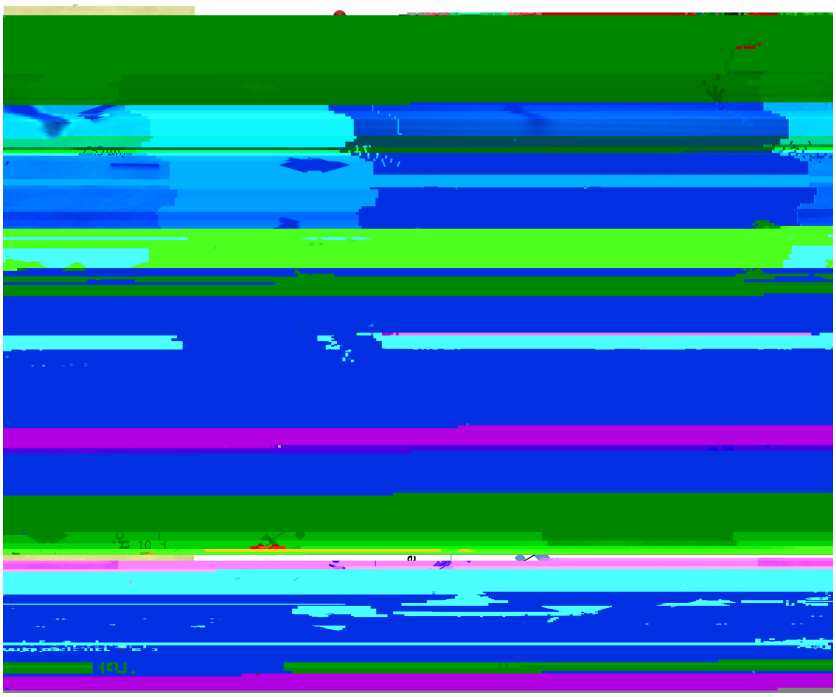

Fig. 2. Vertical translation of a graphene flake across a cholesteric layered structure. (a),(b),(c),(d) Optical micrographs showing an ascending graphene flake suspended in a cholesteric LC when pushed by a defocused laser trap of power ~1 mW, with the focus originally located about 10 μm above the flake. (e) A schematic representation of **n**(**r**) in a cholesteric structure, with the black arrows indicating flake positions along the helical axis χ shown by the blue double arrow (perpendicular to cell substrates and rotating **n** shown by red double arrows). (f),(g) FCPM imaging of the ascent of a graphene flake through the cholesteric

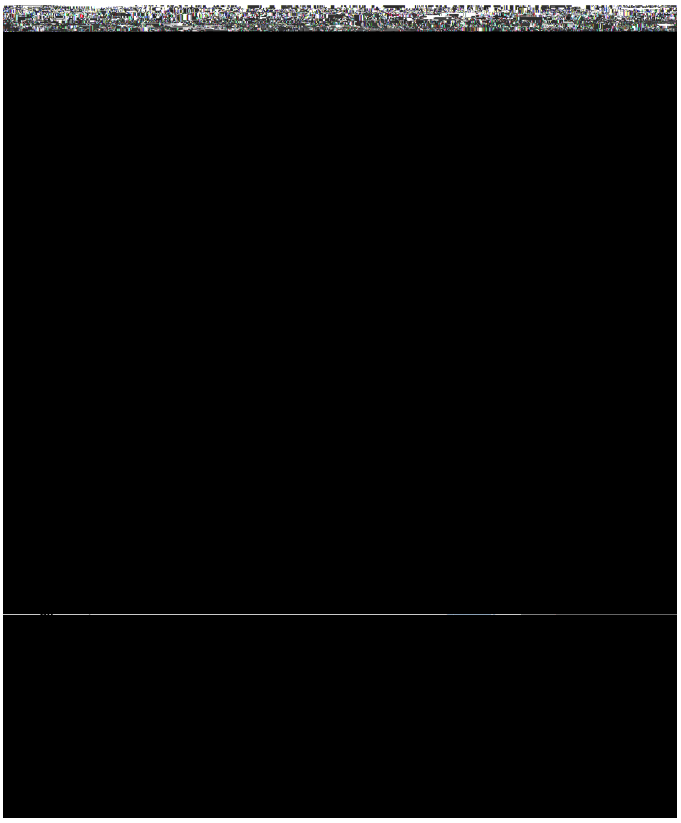

Fig. 3. Laser-induced spinning of a flake in a nematic LC. (a) Optical PM image of a vertically aligned graphene flake in a 20 μm homeotropic nematic cell. (b),(c),(d) Optical PM micrographs showing realignment and rotation of a graphene flake in a laser trap. When the trap is turned on, a vertically aligned flake (b) flips sideways and spins (c-d). The optical images obtained between crossed polarizers highlight the local distortions in the nematic director caused by the spinning graphene flake. The elapsed time is marked on images. (e) A schematic representation of a graphene flake aligned vertically in a homeotropic cell corresponding to the image shown in (a). (f) A schematic representation of a spinning graphene flake and director distortions corresponding to images (c-d); the arrow indicates the spinning direction around the axis normal to the cell substrates. (g) Azimuthal orientation angle of the flake vs. time corresponding to images shown in (c) and (d).

3.2 Non-contact optical manipulation of flakes in nematic and cholesteric liquid crystals

Optical trapping and manipulation of graphene flakes in isotropic fluid hosts, such as water, previously revealed that the interplay between optical and shape anisotropy of these flakes is crucial in determining the alignment and diffusion of graphene in an optical trap [20]. In particular, it was shown that optically trapped submicrometer graphene flakes suspended in water tend to align with the plane of the flake parallel to the light propagation direction and perpendicular to the linear polarization direction [20]. This behavior is in contrast to that of optically trapped transparent platelets and other anisotropic particles that tend to align parallel to the light propagation direction and polarization [6,16]. In LC hosts, however, the trapping behavior is very different as the surface anchoring tends to align the flakes parallel to $\mathbf{n_0}$ and both LC and graphene refractive indices are polarization-dependent. The complex refractive index of graphene in the near infrared part of spectrum is $n_{g\perp} \approx 3 + 1.5i$ for light linearly polarized perpendicular to the graphene's C-axis (parallel to the flake) and $n_{g||} \approx 1.694$ for polarization parallel to the C-axis [20–23]. Both ordinary and extraordinary LC refractive indices are higher than that of water used as a host medium in the previous studies [20] and

#179756 - $15.00 USD Received 12 Nov 2012; revised 24 Dec 2012; accepted 24 Dec 2012; published 11 Jan 2013

3.3 Vertical translation of flakes by scattering forces and measurement of cholesteric pitch

When the laser beam of our HOT setup is focused several micrometers behind a flake, we observe that the flake is pushed across the cell and along the light propagation direction by scattering forces (Fig. 2). If the LC is of cholesteric type with the helical axis normal to the cell substrates, this translation is coupled to rotation of flakes (Fig. 2) [15,16]. When pushed along the helical axis, a flake rotates and follows the helicoidal **n**(**r**), as clearly seen for a low-

structure across the sample thickness and thus also the beam's polarization in the focal plane change as the flake rotates, the transferred optical angular momentum and the rotation rate vary with time [Fig. 3(g)].

3.5 Laser-induced spinning of trapped flakes in a cholesteric LC

The vertical translation of graphene flakes by scattering forces due to a defocused laser beam (Fig. 2) shows that they tend to adopt a well-defined orientation with respect to both the helical axis χ and $\mathbf{n}(\mathbf{r})$ in a planar-aligned cholesteric LC. However, we also find that a trapped graphene flake can spin in both linearly and circularly polarized laser traps (Fig. 4), with the spinning rates being typically at maximum for circularly polarized trapping laser beams and dependent on the flake location in a sample. The spinning rates are constant in time [Fig. 4(a)], linearly increase with the laser power [Fig. 4(b)], and are determined by the competition between the optical and viscoelastic torques exerted on a flake and $\mathbf{n}(\mathbf{r})$-

wior23 Twspi 0 Tw1e144 ond
(i 0 Tw1e1ien)-5(t)1(atio)-5(n)

$\mathbf{n}(\mathbf{r})$-distortions is τ

The otical torque apied to a graphene flake suunded by $_{o} =$ δ δ $\bar{u}$

flakes spin in the laser trap. Since anisotropic nanoparticle spinning effects in linearly polarized trapping laser beams have been also reported for several different types of particles dispersed in isotropic solvents such as water [27–30], it will be of interest to explore how the interplay of anisotropy of a particle (with controlled geometric shapes defined by means of, say, photolithography [31]) and the surrounding medium can be utilized to make these effects even more robust and better controlled, as needed for applications in light-driven micro-machines. A comparative analysis of trapping and spinning behavior of graphene and other anisotropic particles in both isotropic and anisotropic solvents may also provide deeper insights into the physical underpinnings of these phenomena.

4. Conclusion

We have demonstrated translational and rotational non-contact optical manipulation of dispersed self-aligned graphene flakes in both nematic and cholesteric liquid crystals as well as graphene-enhanced realignment of the LC director. Potential applications include optically- and electrically-controlled reconfigurable composites and devices based on ordered LC dispersions of spontaneously aligning colloidal graphene flakes [32]. Our findings may allow for bulk optical patterning of transparent conductive electrodes in the form of interconnected graphene flakes and further expand the applications of graphene in LC-based electro-optic devices and displays [33,34]. We have shown that graphene flakes allow for the realignment of the LC director at threshold laser powers much lower than in graphene-free LCs under otherwise similar conditions. An interesting observation is also the transfer of optical angular momentum from trapping laser beams to flakes in various types of LCs that may be utilized for microrheological studies of these soft matter systems [35].

Acknowledgments

We acknowledge the support of the Institute for Complex Adaptive Matter (ICAM) and the NSF grants DMR-0844115 (C.W.T. and I.I.S.) and DMR-0847782 (J.S.E and I.I.S.). We thank T. Lee, A. Martinez, B. I. Senyuk, and R. P. Trivedi for technical assistance with different aspects of this work. We also acknowledge discussions with N. A. Clark and R. P. Trivedi.

#179756 - $15.00 USD Received 12 Nov 2012; revised 24 Dec 2012; accepted 24 Dec 2012; published 11 Jan 2013